

RESEARCH

Open Access



Conservation genomics of two endangered buntings reveal genetic diversity before and after severe population declines

Shangyu Wang^{1,2†}, Dezhi Zhang^{1†}, Xiaolu Jiao³, Lei Wu^{1,2}, Qiang-Hui Zhu^{1,2}, Hongrui Lv^{1,2}, Haitao Wang⁴, Zheng Han⁴, Shi Li⁵, Peng He^{1,6}, Jun Chen^{1,6}, Shaohong Feng^{7,8,9,10}, Urban Olsson^{11,12}, Per Alström^{1,13} and Fumin Lei^{1,2*}

Abstract

Background Museomics utilizes historical genetic data from museum specimens to inform threatened species conservation. The Yellow-breasted Bunting (*Emberiza aureola*) and the Jankowski's Bunting (*E. jankowskii*), categorized as Critically Endangered or Endangered, respectively, have experienced population declines since the 1970s–1980s. Comparing genetic diversity changes before and after declines is crucial for refining conservation strategies.

Results We de novo assembled genomes for both species and resequenced 29 *E. aureola* (16 historical pre-decline specimens from the 1930s to the 1950s) and 18 *E. jankowskii* (4 historical pre-decline specimens from the 1950s to the 1960s), with 45 individuals from six least-concern *Emberiza* species for comparison. Genetic diversity remained stable in both endangered species from the pre-decline to post-decline periods, with their overall genetic diversity levels being comparable to those of their least-concern congeners. While historically, both had large effective population sizes, *E. jankowskii* showed a gradual decline over 1000 generations, whereas *E. aureola* remained stable. Both modern populations of *E. aureola* and *E. jankowskii* exhibited a higher proportion of long runs of homozygosity (ROH) compared to their historical counterparts, indicating an increased impact of inbreeding following population declines.

Conclusions Despite severe population declines, both species retained high genetic diversity but experienced increased inbreeding. *E. jankowskii* faces ongoing effective population size decline. These insights guide targeted conservation strategies, highlighting the value of museomics in understanding demographic and genetic histories.

Keywords Genetic diversity, Inbreeding, Demography, *Emberiza*

Background

Anthropogenic interference has accelerated the rate of species extinction to an alarming degree [1, 2] and caused losses of species' genetic diversity [3, 4]. The International Union for Conservation of Nature (IUCN) classified more than 47,000 species as threatened with

extinction, accounting for 28% of all assessed species [5]. Nevertheless, genetic information is often overlooked in the IUCN's assessment frameworks [6]. In the past decade, there has been a growing focus on conservation genomic studies targeting an increasing number of endangered species (e.g. [7–9]). Those endangered populations may exhibit low genetic diversity, high inbreeding, and an increased genetic load [10–12], which can reduce individual fitness (e.g. [13, 14]), and render these populations particularly vulnerable to further genetic erosion due to anthropogenic activities [15]. For example, historical population bottlenecks and recent declines

[†]Shangyu Wang and Dezhi Zhang contributed equally to this work.

*Correspondence:

Fumin Lei

leifm@ioz.ac.cn

Full list of author information is available at the end of the article



have led to extremely low genetic diversity and an accumulation of deleterious genetic variations in the Iberian lynx (*Lynx pardinus*) [16]. Similarly, a prolonged 100,000-year population decline has resulted in low genetic diversity and a high proportion of deleterious mutations and homozygous sites in Mountain gorillas (*Gorilla beringei*) [17]. Among avian species, the Southern Dunlin (*Calidris alpina schinzii*) serves as a representative example of declining genetic diversity resulting from habitat fragmentation and population decline [18, 19]. The conservation of the Kakapo (*Strigops habroptilus*) demonstrates that long-term genomic monitoring combined with active management, such as predicting phenotypic traits through breeding values and prioritizing translocations, can help maintain genetic diversity and evolutionary potential even in extremely small populations [20]. These cases underscore the critical importance of integrating genetic information, particularly genome-wide genetic variation [21], into conservation planning to better estimate the extinction risks and inform effective conservation strategies.

Contrary to common assumptions, empirical studies have demonstrated that reduced genetic diversity is not a universal characteristic across all endangered species [22]. For example, a notable avian case is the genomic analysis of the rapidly extinct Carolina parakeet (*Conuropsis carolinensis*), which failed to uncover signs of extended runs of homozygosity or significant historical demographic decline [23]. The critically endangered Coquerel's sifaka (*Propithecus coquereli*) exhibits high heterozygosity despite its population being continuously declining, suggesting that genetic factors may complicate the relationship between historical population dynamics and current genetic diversity [24]. Indian tigers (*Panthera tigris*) have high overall genomic diversity, yet individual tigers have long homozygous segments, possibly due to recent inbreeding or founder effects [25]. Within the Sumatran rhinoceros (*Dicerorhinus sumatrensis*), there are significant differences in genetic diversity among populations [9]. These examples demonstrate that precisely assessing genetic diversity, inbreeding levels, and genetic load serves as the foundation for developing tailored conservation strategies for specific species [16, 26–28].

Notably, museum samples are indispensable for investigating the temporal genetic diversity changes of endangered species [29–32], which in turn facilitates the development of effective conservation strategies and deepens our understanding of population declines [33]. For example, historic specimens of the alpine chipmunk (*Tamias alpinus*) collected in 1915 served as a basis to compare patterns of genetic variation between historical and contemporary populations [34]. A comparison of the historical and modern genomes of the green

peafowl (*Pavo muticus*) revealed a decline in genetic diversity over the past five decades [35], highlighting the impact of human-induced habitat fragmentation on genetic diversity. Analyses of genetic diversity across whole genomes have also shed new light on the historical changes in population size in species recently negatively impacted by humans, such as bird species *Tympanuchus cupido*, *Ectopistes migratorius*, *Campephilus principalis*, *Conuropsis carolinensis*, and *Vermivora bachmanii* [3]. Museum samples enrich our understanding of evolutionary processes of species under human influence [32]. However, despite the valuable insights gained from the above studies, most previous studies on endangered species have relied on partial gene fragments such as microsatellites and mitochondrial markers (e.g., [36]). This emphasizes the need for more in-depth research by using high-quality whole-genome data to explore the changes in genetic diversity and evolutionary potential (e.g., inbreeding depression) before and after population decline. Although some museum genomics studies across temporal scales have emerged (see [33]), such research remains relatively limited.

The Yellow-breasted Bunting (*Emberiza aureola*) and the Jankowski's Bunting (*E. jankowskii*) are classified as Critically Endangered or Endangered, respectively, on the IUCN Red List [5], due to significant population declines observed over the past few decades. Historically, *E. aureola* was widely distributed across the Eurasian continent. However, due to excessive human hunting, its western boundary of distribution range has shifted eastward by approximately 5000 km from 1980 to 2013, and its population has declined by over 90% since the 1980s [37]. The demand for *E. aureola* in the traditional food market, particularly in some regions of China, has led to large-scale and unsustainable hunting [38, 39]. Nevertheless, despite having undergone a severe population decline, the Yellow-breasted Bunting still maintains high genetic diversity, exhibits low linkage disequilibrium, and shows a low proportion of long runs of homozygosity [40]. In contrast, the distribution of *E. jankowskii* is relatively restricted. This species primarily inhabits meadows and thickets in Northeast China, as well as adjacent areas of Mongolia and the Russian Far East [41]. The breeding population of *E. jankowskii* has experienced a continuous and significant decline since the 1970s [42]. Currently, its relict breeding range is restricted to the steppes in Jilin Province and several counties in Inner Mongolia, with suitable breeding habitat covering only 280 km² [43]. Over the past 50 years, it has vanished from most of its historical breeding sites [42]. In 2018, the global population was estimated at 9800–12,500 individuals [44]. Intriguingly, compared with other avian species, *E. jankowskii* exhibits unexpectedly high levels of genetic

diversity in both mitochondrial DNA and microsatellites [45, 46].

However, the patterns of genetic diversity change in these two endangered species before and after their population declines remain poorly understood. In this study, we assembled two high-quality reference genomes for both species. By utilizing historical museum specimens and contemporary samples, we retrieved genomic data spanning both pre-decline (1930s, 1950s and 1960s) and post-decline (2000s and 2010s) periods. Integrating historical and contemporary genetic data, this study quantified genetic diversity through heterozygosity, measured inbreeding using runs of homozygosity (ROH), and reconstructed demographic history, thereby providing insights into the conservation status of the two endangered species.

Results

De novo assembly of the genome of *E. aureola* and *E. jankowskii*

Based on the stLFR sequencing libraries and the BGISEQ-500 high-throughput sequencing platform [47], we assembled the genomes of these two species at the Beijing Genomics Institute (Shenzhen, China). The assembled genome of *E. aureola* has a length of 1.09 Gb and consists of 33,220 scaffolds. The N50 value of this genome is 8.2 Mb, and the largest scaffold is 40.89 Mb.

The assembled genome of *E. jankowskii* has a length of 1.07 Gb and comprises 40,940 scaffolds. The N50 value of this genome is 0.61 Mb, and the largest scaffold is 6.12 Mb (Additional file 2: Table S1). Based on the evaluation using benchmarking universal single-copy orthologs (BUSCO) (passeriformes_odb10), the assembly completeness levels for *E. aureola* and *E. jankowskii* were assessed at 92.7% and 89.4%, respectively, which indicates high quality of assembly (Additional file 1: Fig. S1).

Whole-genome resequencing and grouping

We sequenced 29 individuals for *E. aureola*, comprising 16 historical specimens (collected from the 1930s to the 1950s) and 13 modern samples (collected from the 2000s to the 2010s). For *E. jankowskii*, we sequenced 8 individuals, including 4 historical specimens (collected from the 1950s to the 1960s) and 4 modern samples (collected from the 2000s to the 2010s), and further integrated data from 10 previously published modern individuals (Fig. 1; Additional file 2: Table S2). To enable a comprehensive comparison, we incorporated genomic data from six additional *Emberiza* species, which are all classified as Least Concern: 8 individuals each of Godlewski's Bunting (*E. godlewskii*), Rock Bunting (*E. cia*), Meadow Bunting (*E. cioides*), Yellow-throated Bunting (*E. elegans*), and Chestnut Bunting (*E. rutila*), as well as 5 individuals of White-capped Bunting (*E. stewarti*). In total, our

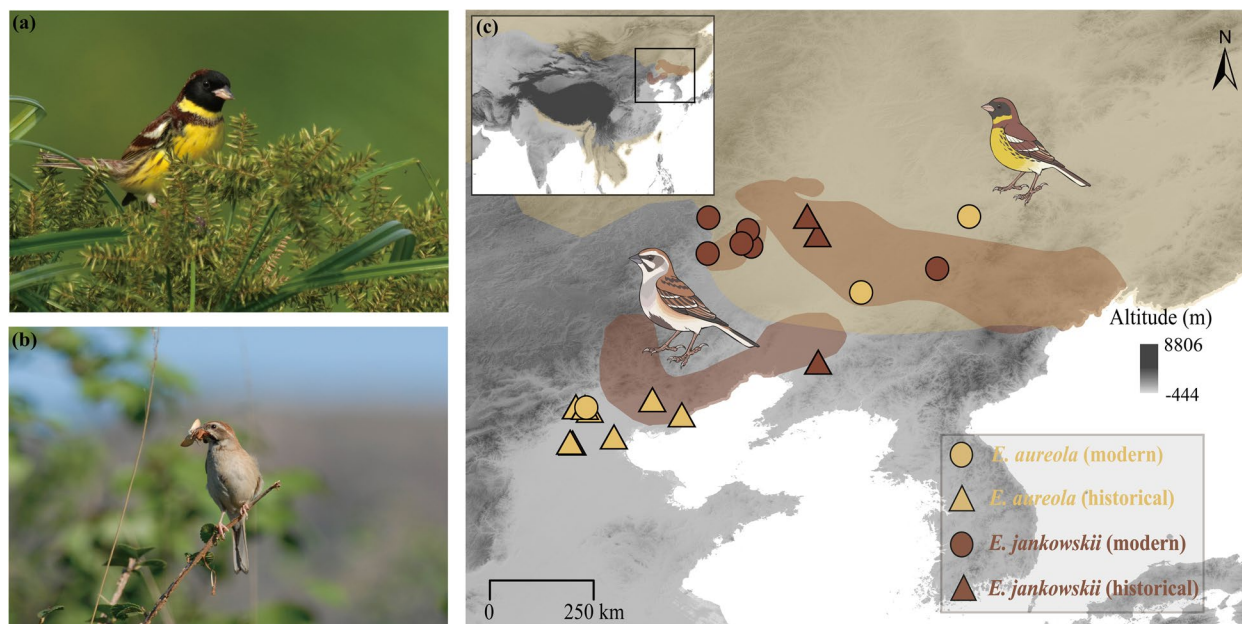


Fig. 1 Ecological photos and distribution of sampling sites. **a** *E. aureola* (photographed by Xingbin Yang). **b** *E. jankowskii* (photographed by Haitao Wang). **c** The yellow color represents *E. aureola* and the brown color represents *E. jankowskii*. The two hand-drawn pictures depict two male individuals. Each shape represents a single sampling site. Different shapes represent different groups of sampling periods. The distribution range is demarcated by shading, with the data sourced from BirdLife (<https://www.birdlife.org/>). The top left inset represents the study area. The map is the elevation data downloaded from WorldClim (<http://www.worldclim.org>)

dataset comprises 50 newly re-sequenced genomes and 42 genomes from two previous studies (Additional file 2: Table S2) [42, 43]. After trimming and mapping the reads to the reference genome, we excluded 4 low-quality historical *E. aureola* individuals with a sequencing depth of less than 5 \times . After filtering, the remaining dataset exhibited an average sequencing depth of 16.1 \times , a breadth of coverage of 93.0%, and a mean mapping rate of 96.7%. To explore potential temporal trends in genetic variation, we categorized the samples of *E. aureola* and *E. jankowskii* into two period groups according to their sampling dates (before and after the population decline) (Additional file 2: Table S2).

Genetic diversity of *E. aureola* and *E. jankowskii*

Multiple established metrics are available for quantifying genetic diversity of populations, including nucleotide diversity, haplotype diversity, haplotype richness, and heterozygosity [48]. Here, we used heterozygosity as a proxy of genetic diversity, calculated as the proportion of heterozygous sites per individual. Our results reveal that both *E. aureola* and *E. jankowskii*, despite having undergone significant population declines, exhibit higher levels of genomic heterozygosity compared to most of their relatives (Fig. 2a). Before and after the rapid population decline, no significant loss of genetic diversity was found in either of the two species (Fig. 2b and Additional file 1: Fig. S2). For *E. aureola*, regardless of whether the samples were categorized into four groups based on sampling decades or divided into historical and modern periods, no significant differences in genetic diversity were detected (Fig. 2b and Additional file 1: Fig. S2). This suggests that the genetic diversity of *E. aureola* has remained relatively stable over time. For *E. jankowskii*, genetic diversity in the modern population was slightly higher than that in the historical one, although this difference was not statistically significant (Fig. 2b and Additional file 1: Fig. S2). We also constructed the linkage disequilibrium (LD) decay curve for these species. *E. aureola* and *E. jankowskii* exhibited a lower degree of LD compared to other Least Concern relatives (Additional file 1: Fig. S3).

Inbreeding of *E. aureola* and *E. jankowskii*

Runs of homozygosity (ROH) were used to represent the inbreeding level of the two endangered species. ROH arise from the mating of closely related individuals. When closely related individuals mate, the offspring inherit long genomic segments that are homozygous and identical by descent [49]. Long ROH are typically indicative of recent inbreeding, whereas shorter ROH suggest ancestry from more distant common ancestors. Calculating the proportions of an individual's genome that occurs

as ROH of specific lengths may provide insights into the extent of inbreeding [50]. We calculated the number of long (>1000 kb) and short (300–1000 kb) ROHs, as well as the percentage contribution of each type of ROH [51]. We also calculated the ROH of *E. elegans* for comparison. Specifically, among the 14 examined modern individuals of *E. jankowskii*, ROH segments with lengths exceeding 300 kb were successfully identified. The average length of these detected ROH segments was approximately 485.3 kb (Additional file 1: Fig. S4a). Segments longer than 1,000 kb accounted for approximately 6% of the total identified segments (Fig. 3a). For the historical specimens of *E. jankowskii*, 4 individuals were investigated. The average length of ROH segments exceeding 300 kb was 427.5 kb (Additional file 1: Fig. S4a). None of the identified segments in these historical individuals exceeded 1000 kb in length, suggesting a different distribution of long ROH segments between modern and historical *E. jankowskii* populations (Additional file 1: Fig. S4b). Among the 13 modern individuals examined of *E. aureola*, the average length of ROH segments exceeding 300 kb was 684.4 kb (Additional file 1: Fig. S4a). Moreover, ROH segments longer than 1000 kb constituted approximately 16.4% of the total detected segments (Fig. 3a), indicating a higher proportion of long homozygous regions, and a greater length of these regions, in modern *E. aureola* than in modern *E. jankowskii*. In the 12 historical individuals of *E. aureola*, approximately 13.8% of these segments were longer than 1000 kb (Fig. 3a), and the average length of all detected ROH segments was approximately 615.8 kb (Additional file 1: Fig. S4a). These findings suggest that, while there are similarities in the presence of long ROH segments between modern and historical *E. aureola* populations, there are also differences in their proportion and average length (Additional file 2: Table S4). In both species, the cumulative length of short ROH segments was higher than that of long ROH segments. Within *E. jankowskii*, the distribution of ROH among individuals was uneven. Four modern samples exhibited a high number of ROH (more than 55 per individual). For comparison, the average number of ROH per individual was only 2 in the four historical sample groups, compared to 11 per individual among the other modern samples. In contrast, the number of ROH in *E. aureola* was relatively consistent across individuals (Fig. 3b and Additional file 2: Table S5). Overall, modern populations of *E. aureola* and *E. jankowskii* exhibit a larger average length of ROH and a higher proportion of long ROH compared to their historical populations, indicating a higher degree of inbreeding in the modern populations.

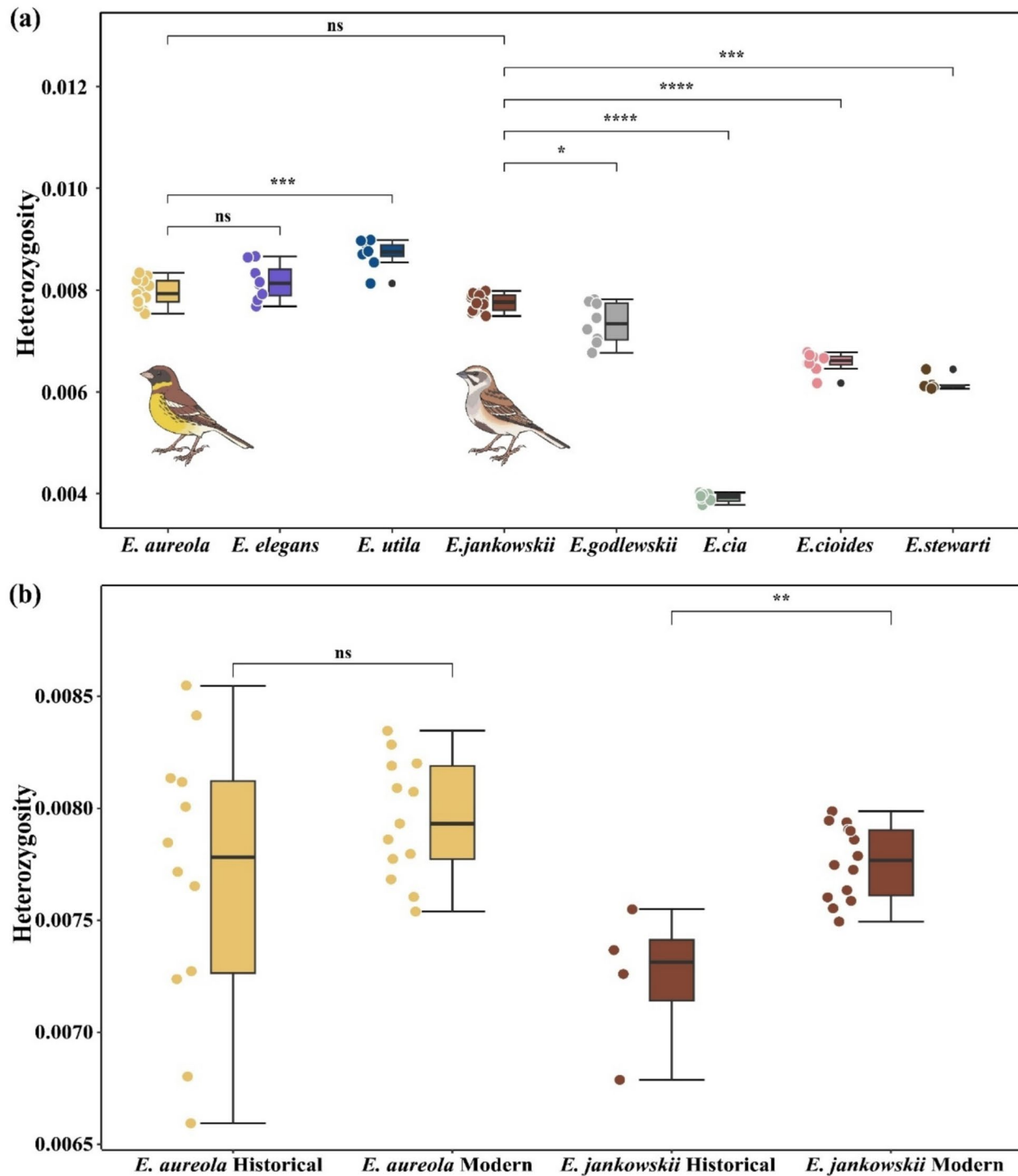


Fig. 2 Genetic diversity and inbreeding. **a** Comparison of heterozygosity between eight species in genus *Emberiza* using the Wilcoxon rank-sum test (for *E. aureola* and *E. jankowskii*, only modern samples are included). **b** Comparison of heterozygosity between historical and modern individuals in *E. aureola* and *E. jankowskii*. (**** $P < 0.001$, ** $P < 0.01$, * $P < 0.05$, and NS is not significant)

Demography of *E. aureola* and *E. jankowskii*

We employed two distinct approaches to reconstruct the demographic history of *E. aureola* and *E. jankowskii*.

The Pairwise Sequentially Markovian Coalescent (PSMC) method was used to infer the long-term historical demography [52]. The results estimated from the

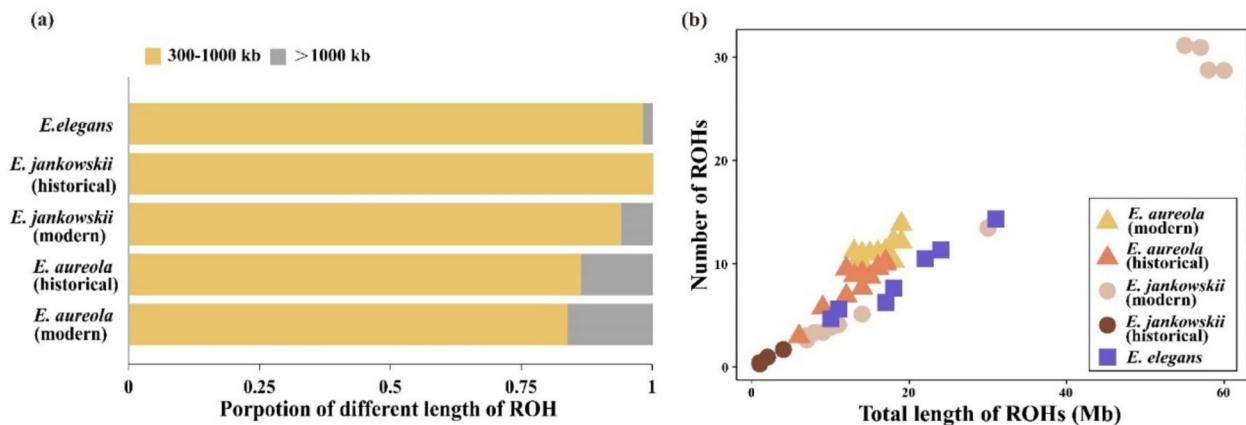


Fig. 3 Inbreeding. **a** Proportion of different lengths of ROHs in *E. aureola*, *E. jankowskii*, and *E. elegans*. The yellow part represents short ROHs of 300–1000 kb, and the grey part represents long ROH ≥ 1000 kb. **b** The number and total length of ROH in *E. aureola*, *E. jankowskii*, and *E. elegans*

individual with the highest sequencing depth for each species (9319, ALH01, LW23576, 20298, 21435, 20360, 24332, 23939) show that the historical effective population sizes of *E. aureola* and *E. jankowskii* were comparable to some least-concern species (Fig. 4a). *E. aureola* experienced a continuous population contraction from approximately 4×10^5 years ago, while *E. jankowskii* exhibited a trend of gradual population growth since approximately one million years ago (Fig. 4a). The same analysis conducted on other individuals with a sequencing depth of greater than $15\times$ also supports this trend (Additional file 1: Fig. S5). Stairway Plot was used to detect recent demographic changes in *E. aureola* and *E. jankowskii* (Fig. 4b and c) [53]. According to this, both species underwent demographic contraction followed by expansion between 60,000 and 20,000 generations ago. Since then, the effective population size of *E. aureola* has remained largely stable (Fig. 4b), whereas that of *E. jankowskii* has continued to decline, eventually reaching approximately one-sixth of its historical peak (Fig. 4c).

Discussion

Comparing genetic changes between a historical population before a population decline with that after the decline will provide important references for the conservation of endangered species [54, 55]. However, most existing studies focus on comparisons across different periods [34, 35] or only on changes in genetic diversity after population decline [56]. Studies of the changes before and after population decline are rarely conducted [54, 57]. In our study, comparing the genomes of two endangered species, both before and after their population declines, we did not find that the significant population decline led to a reduction in their genetic diversity, but a certain increase in their inbreeding level.

Our results have revealed that the Critically Endangered species *E. aureola* and the Endangered *E. jankowskii* both exhibit a relatively high level of genetic diversity compared to other least-concerned *Emberiza* species (Fig. 2a). The results comparing the genetic diversity of *E. aureola* and *E. jankowskii* before and after their rapid population decline also suggest that no significant changes in their genetic diversity have occurred (Fig. 2b and Additional file 1: Fig. S2). This result confirms the previous genomic study of *E. aureola* [40] and the studies on mitochondria and microsatellites of *E. jankowskii* [46, 58]. Although genetic diversity is an important indicator of species endangerment, there is no strict correspondence between genetic diversity and the IUCN Red List status [59, 60]. Unlike other endangered species such as the Passenger Pigeon (*Ectopistes migratorius*), which experienced rapid population decline from large numbers alongside extremely low genetic diversity, the two endangered species in this study show distinct patterns [61, 62]. Both species have undergone recent rapid population decline, yet neither experienced a reduction in genetic diversity, which may have various causes [63]. For instance, their historical population sizes might have been large enough to endow them with a substantial genetic reservoir, such as the high genetic diversity observed in the Critically Endangered California Condor (*Gymnogyps californianus*) [64]. Similarly, the Roseate Tern (*Sterna dougallii*) also experienced range contractions and population declines due to anthropogenic activities in the twentieth century, but no change in its genetic diversity over time was detected [65]. Some studies have shown that there is a lag between changes in population size and genetic diversity, where after a severe decline in population size, genetic diversity may continue to be

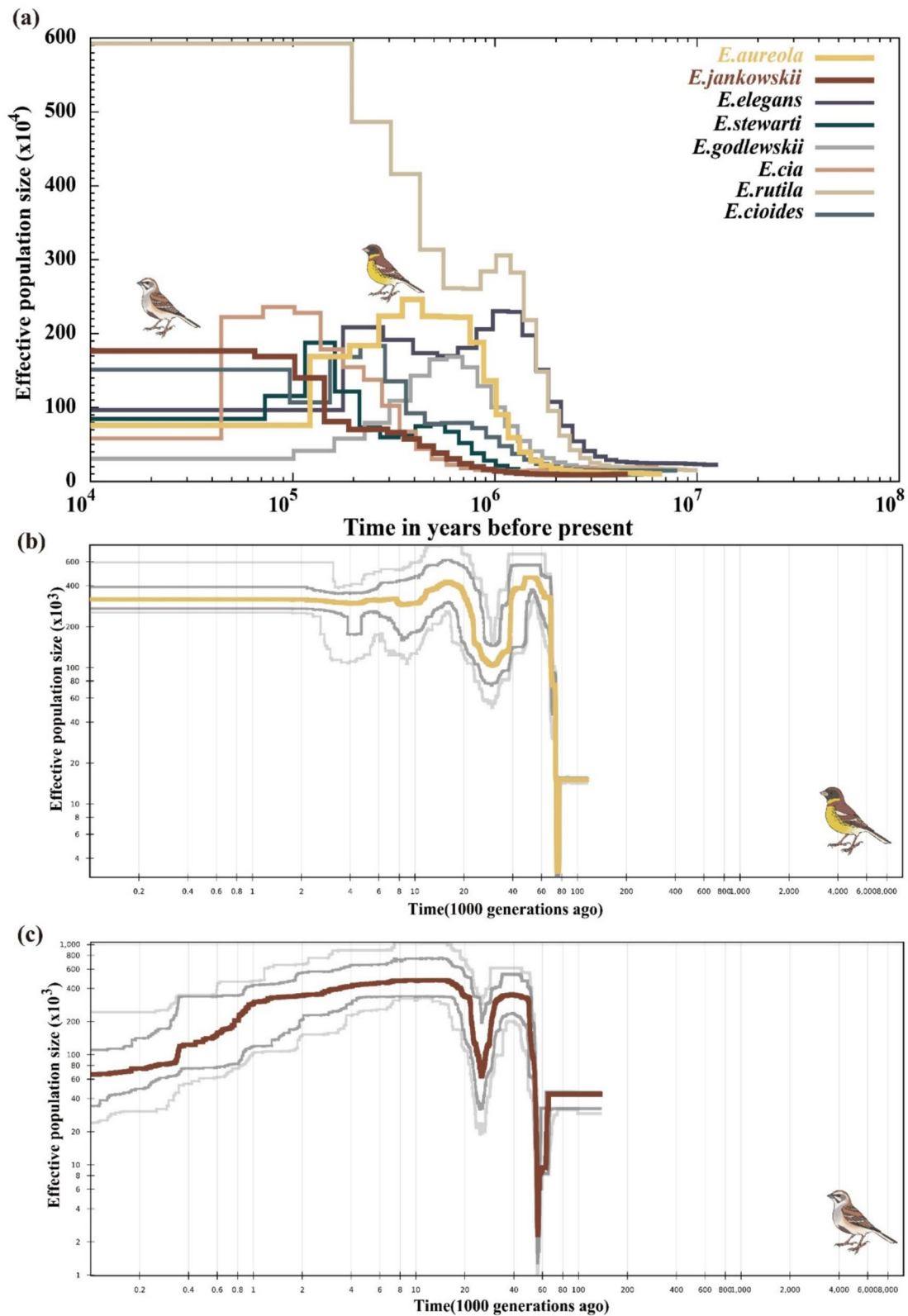


Fig. 4 Demographic history reconstruction. **a** PSMC reconstruction of the past demographic history for eight species in genus *Emberiza*. Stairway plots estimate the recent change of effective population size in *E. aureola* **(b)** and *E. jankowskii* **(c)**

lost even when the population stabilizes or increases [66]. In the context of our study species, this lag could imply that the current genetic diversity may not accurately reflect their recent population declines. It is possible that a future reduction in genetic diversity might still occur as the lagged effects take hold, warranting long-term monitoring.

Although there is no evidence of reduced genetic diversity, the two endangered bunting species exhibit an elevated level of ROHs compared to *E. elegans* (Fig. 3), indicating a trend towards inbreeding depression, which may cause a decrease of fitness [67–69]. In both species, short ROH segments were more prevalent, but modern populations had a longer average ROH and a higher proportion of long ROH segments compared to historical populations, indicating increased inbreeding (Fig. 3a). Moreover, *E. jankowskii* showed substantial inter-individual variation in ROH number, while *E. aureola* had more consistent ROH patterns (Fig. 3b). Overall, these findings suggest elevated inbreeding levels in the modern populations of these two endangered species. Inbreeding depression associated with population decline has also been observed in the Critically Endangered Siberian Crane (*Leucogeranus leucogeranus*) [51]. Although purifying selection may counteract some detrimental effects of inbreeding depression, evidence suggests that remaining deleterious alleles may still impose fitness costs associated with inbreeding [70–72].

Despite human disturbance causing severe population declines, *E. aureola* and *E. jankowskii* have retained relatively high genetic diversity across pre- and post-decline periods. This finding offers hope for the future population recovery of these endangered species and provides a reference for conservation planning. It highlights that for species with strong recovery potential, targeted conservation strategies may effectively facilitate population restoration.

Conclusions

In this study, we systematically investigated the temporal changes in genetic diversity of two endangered bird species by comparing genomic data from populations before and after declines. We demonstrate that the genetic diversity of these two endangered species remains relatively high compared to non-endangered congeneric species. Furthermore, despite the significant decline in their populations over recent decades, genetic diversity has not decreased; nonetheless, the levels of inbreeding have increased. Our study provides a new case study of endangered species with substantial recovery potential and establishes a theoretical foundation for formulating targeted, species-specific conservation strategies.

Methods

De novo assembly of the genome of *E. aureola* and *E. jankowskii*

In this study, we performed de novo sequencing and assembly of the draft genomes of a male *E. aureola* and a male *E. jankowskii* (sample IDs: IOZ_3392 and IOZ_4549) (Additional file 2: Table S1). We used the RecoverEase DNA Isolation Kit for DNA extraction. The single tube long fragment read (stLFR) sequencing libraries were constructed for each species following the manufacturer's protocols [47] and subsequently sequenced on the BGISEQ-500 high-throughput sequencing platform with a paired-end read length of 100 base sbp. The raw reads were filtered in SOAPfilter2 v.2.2 package [73] using the following steps: firstly, reads with more than 10% of N bases were removed; secondly, reads containing more than 40% of low-quality bases (with a Phred score ≤ 10) were eliminated; thirdly, reads with an undersized insert size were discarded; finally, Polymerase Chain Reaction duplicates were filtered out (if read1 and read2 of the same paired-end reads were identical, they were regarded as duplicates). The clean stLFR reads were converted into the 10X Genomics linked-reads format [74] and used as input for Supernova v.2.0.1 [73] in pseudohap mode for genome assembly of each sample. Following the preliminary assembly, scaffolds containing more than 80% "N" bases were removed. Subsequently, GapCloser2 v.1.12 [75] was employed to close the intra-scaffold gaps, thus completing the refinement of the genome assembly. Library preparation, sequencing, and assembly were conducted at Beijing Genomics Institute (Shenzhen, China). The completeness of the assemblies was evaluated using the passeriformes_odb10 database by BUSCO v.5.7.0 [76, 77] with default parameters.

Sampling, whole-genome resequencing, and variant calling

We sampled a total of 50 individuals, including 29 individuals of *E. aureola*, 8 individuals of *E. jankowskii*, 8 individuals of *E. rutila*, and 5 individuals of *E. stewarti* deposited in the Institute of Zoology, Chinese Academy of Sciences, Beijing (Additional file 2: Table S2). Total genomic DNA was extracted from tissue, blood, or toepad using the DNeasy blood and tissue kit (Qiagen) according to the manufacturer's protocol. DNA libraries with ~ 350 bp inserts were constructed and sequenced using the Illumina NovaSeq 6000 platform with a PE read length of 150 bp. Raw reads were processed to remove adapter sequences, low-quality reads (those with over 50% of bases having Phred quality scores < 3) and poly-N reads (those with $\geq 3\%$ unidentified nucleotides) using fastp v.0.20.0 [78]. Additionally, we incorporated published sequencing data from

10 individuals of *E. jankowskii*, 8 individuals of *E. godlewskii*, 8 individuals of *E. cia*, 8 individuals of *E. cioides*, and 8 individuals of *E. elegans* (NCBI BioProject: PRJNA797667 and PRJNA751503) (Additional file 2: Table S2) [79, 80]. Previous phylogenetic analyses have delineated the evolutionary relationships among these species, indicating that *E. aureola*, *E. rutila*, and *E. elegans* share a most recent common ancestor, while the remaining five species form a distinct clade [81]. According to the phylogenetic relationship, quality-controlled reads of samples were mapped to the following reference genome: samples of *E. aureola* and *E. rutila* were mapped to the newly assembled *E. aureola* genome, samples of *E. jankowskii*, *E. stewartii*, *E. godlewskii*, *E. cia*, and *E. cioides* were mapped to the newly assembled *E. jankowskii* genome, and samples of *E. elegans* were mapped to its own genome (GenBank genome assembly accession: GCA_022818055.1 [79]) using BWA 0.7.12 with mem command [82]. For museum samples, mapDamage v.2.0 was used for rescaling using “-rescale” option [8]. The sequencing depth and breadth of coverage for each sample were estimated using BEDtools v.2.27 with “genomecov” function [83]. We removed 4 individuals of *E. aureola* with a sequencing depth of less than 5× because the relatively low sequencing depth and coverage of individuals from historical periods may have exerted a certain impact on the calculation of heterozygosity. Mapping rates were estimated by picard-tools v.1.96 (<https://broadinstitute.github.io/picard/>). Variants were called in SAMtools v.0.1.19 using the “mpileup” module [84]. Single nucleotide polymorphism (SNPs) were filtered using VCFtools v.0.1.13 [85] according to the following criteria: (i) quality value ≥ 30 ; (ii) genotype depth $\geq 5 \times$; (iii) only biallelic SNPs were retained; (iv) SNPs with ≥ 9 missing genotypes across all individuals were removed.

Estimating genetic diversity and linkage disequilibrium

Heterozygosity was used as a proxy of genetic diversity. Consensus fasta sequences were generated using SAMtools v.0.1.19 [84] and BCFtools v.1.3.1 [82], with a minimal sequencing depth of 5 × and a maximal sequencing depth of 100. Heterozygosity of each individual was calculated as the ratio of heterozygous sites to total variant sites, i.e., “Heterozygosity = number of heterozygous SNPs / (number of heterozygous SNPs + number of homozygous SNPs)” in the resulting consensus sequence (Additional file 2: Table S3) [79]. We calculated the correlation coefficient (r^2) of LD pattern using PopLDdecay v.3.4 [86], setting the maximum distance between two SNPs to 20 kb. Only modern samples were used for LD analysis.

Estimating inbreeding pattern

ROH was used to evaluate the level of inbreeding. To infer the number and length of ROH, we first used VCFtools v.0.1.13 [85] to convert variant call format file to PLINK ped and map format. Subsequently, we used plink v.1.90 [87] to identify ROH larger than 300 kb with the following parameters: -homozyg -homozyg-density 50 -homozyg-gap 100 -homozyg-kb 300 -homozyg-snp 50 -homozyg-window-het 3 -homozyg-window-snp 50 -homozyg-window-threshold 0.05 [40]. Long ROHs (>1,000 kb) are typically generated by recent ancestors, while recombination can break the ROH, making short ROHs (<1000 kb) more likely to have originated from distant ancestors [49, 50]. We calculated the number of short ROH (300–1000 kb) and long ROH (>1000 kb) and the percentage of the two kinds of ROH [51].

Inference of demographic history

We used two methods to reconstruct demographic history from ancient to recent times. We inferred past effective population size from individual whole-genome sequences using PSMC [88]. Considering the influence of sequencing depth on PSMC analysis [52], we restricted our analyses to individuals with a sequencing depth greater than 15× across the eight species (sampling numbers: 9319, ALH01, LW23576, 20298, 21435, 20360, 24332, and 23939; Additional file 2: Table S2). Among these, all but *E. cioides* (sequencing depth of 16.1×) had a sequencing depth greater than 18×, ensuring relatively high data quality (Additional file 2: Table S2). Additionally, for intraspecific comparisons, we used all individuals with a sequencing depth greater than 15× (Additional file 1: Fig. S5). The PSMC v.0.6.5 was performed using the following settings: -N25 -t15 -r5 -p"4+25*2+4+6". The mutation rate was set to 2×10^{-9} per site per year, and the generation time was specified as 2 years [79]. For *E. aureola* and *E. jankowskii*, we performed 100 bootstrap replicates. Given the limited resolution of PSMC, which does not provide information on recent N_e , we used Stairway Plot v.2.1.1 to produce more precise inferences for recent N_e changes [53, 89]. Stairway Plot leverages information from the site frequency spectrum (SFS) to reconstruct past demographic dynamics [53, 90]. We used ANGSD v.0.910 with the -doSaf 1 option to calculate site allele frequency Likelihoods and employed the realSFS tool with the -maxIter 100 parameter to generate the folded SFS [91]. The folded SFS file was used as an input file for Stairway Plot analysis, with a mutation rate of 2×10^{-9} per site per generation and a consistent generation time of 2 years. The effective population

size through time was estimated using default training settings, which utilized 67% of the sites, and 95% confidence intervals were calculated based on 100 replicates.

Abbreviations

BUSCO	Benchmarking Universal Single-Copy Orthologs
IUCN	International Union for Conservation of Nature
LD	Linkage disequilibrium
PSMC	Pairwise Sequentially Markovian Coalescent
ROH	Runs of homozygosity
SFS	Site frequency spectrum
SNP	Single nucleotide polymorphism
stLFR	Single tube long fragment read

Supplementary Information

The online version contains supplementary material available at <https://doi.org/10.1186/s12915-025-02393-7>.

Additional file 1: Figures S1–S5. Fig. S1. BUSCO assessment results for the de novo reference genome of *E. aureola* and *E. jankowskii*. Fig. S2. Comparison of heterozygosity between each historical and modern group in *E. aureola* and *E. jankowskii*. Fig. S3. Linkage disequilibrium decay within 20 kb of seven species in genus *Emberiza*. Fig. S4. All ROHs longer than 300kb in *E. aureola*, *E. jankowskii*, and *E. elegans*. Fig. S5. PSMC reconstruction of the past demographic history for individuals with sequencing depths of more than 15x from eight *Emberiza* species.

Additional file 2: Tables S1–S5. Table S1. Information of *E. aureola* and *E. jankowskii* genome assembly. Table S2. Sample information, sequencing and alignment Details. Table S3. Heterozygosity of each individual. Table S4. Information of all the ROHs. Table S5. Total ROHs in each individual.

Acknowledgements

Many thanks to the editors and two anonymous reviewers for constructive suggestions for improving the manuscript. We thank Xingbin Yang for providing the photo of the Yellow-breasted Bunting. We thank Xinwen Yang for drawing the bird illustrations for this paper. We also thank the National Animal Collection Resource Center, Institute of Zoology, Chinese Academy of Sciences, for assistance in specimen examination.

Authors' contributions

This study was designed by F.L. and D.Z. The data were analyzed by S.W., D.Z., X.J., L.W., Q.Z., S.F. and H.L. Field work and sample collections were conducted by F.L., S.W., H.W., P.H., J.C., Z.H. and S.L. The manuscript was written by S.W., D.Z., P.A., U.O. and F.L. and commented on and approved by all authors. All authors read and approved the final manuscript.

Funding

This research was funded by the National Science Foundation of China (32270466 to D.Z., 32130013 to F.L.); the Youth Innovation Promotion Association CAS (2023093 to D.Z.); the National Key Research and Development Program of China (2022YFC2601601 to F.L.); the Institute of Zoology, Chinese Academy of Sciences (2023IOZ0104 to F.L.); and the Swedish National Science Foundation (2019–04486) and Jorvall Foundation (to P.A.).

Data availability

The genome assembly of **E. aureola** and **E. jankowskii** have been deposited to the National Genomics Data centre (<https://db.cngb.org/>) with accession number CNP0007710 and are available at the following URL: <https://doi.org/10.26036/CNP0007710> [92]. The whole genome sequencing data generated in this study has been deposited into the NCBI Sequence Read Archive under a BioProject portal of PRJNA1264757 and are available at the following URL: <https://www.ncbi.nlm.nih.gov/bioproject/PRJNA1264757> [93].

Declarations

Ethics approval and consent to participate

Not applicable.

Consent for publication

Not applicable.

Competing interests

The authors declare no competing interests.

Author details

¹State Key Laboratory of Animal Biodiversity Conservation and Integrated Pest Management, Institute of Zoology, Chinese Academy of Sciences, Beijing 100101, China. ²College of Life Sciences, University of Chinese Academy of Sciences, Beijing 100049, China. ³Hebei Key Laboratory of Animal Physiology, Biochemistry and Molecular Biology, College of Life Sciences, Hebei Normal University, Shijiazhuang 050024, China. ⁴School of Life Sciences, Jilin Engineering Laboratory for Avian Ecology and Conservation Genetics, Northeast Normal University, Changchun 130024, China. ⁵College of Animal Science and Technology, Jilin Agricultural University, Changchun 130118, China. ⁶Institute of Zoology, National Animal Collection Resource Center, Chinese Academy of Sciences, Beijing 100101, China. ⁷Center for Evolutionary and Organismal Biology, Zhejiang University School of Medicine, Hangzhou, China. ⁸Liangzhu Laboratory, Zhejiang University Medical Center, Hangzhou, China. ⁹Department of General Surgery of Sir Run Run Shaw Hospital, Zhejiang University School of Medicine, Hangzhou, China. ¹⁰Innovation Center of Yangtze River Delta, Zhejiang University, Hangzhou, China. ¹¹Department of Biology and Environmental Science, University of Gothenburg, Box 463, 405 30 Gothenburg, Sweden. ¹²Gothenburg Global Biodiversity Centre, Box 461, 405 30 Gothenburg, Sweden. ¹³Animal Ecology, Department of Ecology and Genetics, Evolutionary Biology Centre, Uppsala University, Norbyvägen 18 D, 752 36 Uppsala, Sweden.

Received: 20 May 2025 Accepted: 21 August 2025

Published online: 01 October 2025

References

- Ceballos G, Ehrlich PR. Mutilation of the tree of life via mass extinction of animal genera. *Proc Natl Acad Sci U S A*. 2023;120(39):e2306987120.
- Urban MC. Climate change extinctions. *Science*. 2024;386(6726):1123–8.
- Smith BT, Gehara M, Harvey MG. The demography of extinction in eastern North American birds. *Proc Biol Sci*. 2021;288(1944):20201945.
- Exposito-Alonso M, Booker TR, Czech L, Gillespie L, Hately S, Kyriazis CC, et al. Genetic diversity loss in the anthropocene. *Science*. 2022;377(6613):1431–5.
- IUCN. 2024. The IUCN Red List of Threatened Species. Version 2024–2. <https://www.iucnredlist.org>. Accessed on 20 Mar 2025.
- Willi Y, Kristensen TN, Sgro CM, Weeks AR, Ørsted M, Hoffmann AA. Conservation genetics as a management tool: The five best-supported paradigms to assist the management of threatened species. *Proc Natl Acad Sci U S A*. 2022;119(1):e2105076119.
- Scott PA, Allison LJ, Field KJ, Averill-Murray RC, Shaffer HB. Individual heterozygosity predicts translocation success in threatened desert tortoises. *Science*. 2020;370(6520):1086.
- Feng S, Fang Q, Barnett R, Li C, Han S, Kuhlwlilm M, et al. The genomic footprints of the fall and recovery of the crested ibis. *Curr Biol*. 2019;29(2):340.
- von Seth J, Dussex N, Diez-del-Molino D, van der Valk T, Kutschera VE, Kierczak M, et al. Genomic insights into the conservation status of the world's last remaining Sumatran rhinoceros populations. *Nat Commun*. 2021;12(1):2393.
- Wang P, Burley JT, Liu Y, Chang J, Chen D, Lu Q, et al. Genomic consequences of long-term population decline in brown eared pheasant. *Mol Biol Evol*. 2021;38(1):263–73.
- Yang L, Wei F, Zhan X, Fan H, Zhao P, Huang G, et al. Evolutionary conservation genomics reveals recent speciation and local adaptation in threatened takins. *Mol Biol Evol*. 2022;39(6):msac111.

12. Gu T-T, Wu H, Yang F, Gaubert P, Heighton SP, Fu Y, et al. Genomic analysis reveals a cryptic pangolin species. *Proc Natl Acad Sci U S A*. 2023;120(40):e2304096120.
13. Westemeier RL, Brawn JD, Simpson SA, Esker TL, Jansen RW, Walk JW, et al. Tracking the long-term decline and recovery of an isolated population. *Science*. 1998;282(5394):1695–8.
14. Markert JA, Champlin DM, Gutjahr-Gobell R, Grear JS, Kuhn A, McGreevy TJ Jr, et al. Population genetic diversity and fitness in multiple environments. *BMC Evol Biol*. 2010;10:205.
15. Zou D, Tian S, Zhang T, Zhuoma N, Wu G, Wang M, et al. Vulture genomes reveal molecular adaptations underlying obligate scavenging and low levels of genetic diversity. *Mol Biol Evol*. 2021;38(9):3649–63.
16. Abascal F, Corvelo A, Cruz F, Villanueva-Canas JL, Vlasova A, Marcet-Houben M, et al. Extreme genomic erosion after recurrent demographic bottlenecks in the highly endangered Iberian lynx. *Genome Biol*. 2016;17(1):251.
17. Xue Y, Prado-Martinez J, Sudmant PH, Narasimhan V, Ayub Q, Szpak M, et al. Mountain gorilla genomes reveal the impact of long-term population decline and inbreeding. *Science*. 2015;348(6231):242–5.
18. Blomqvist D, Pauliny A, Larsson M, Flodin L-A. Trapped in the extinction vortex? Strong genetic effects in a declining vertebrate population. *BMC Evol Biol*. 2010;10:33.
19. Ronka N, Pakanen V-M, Pauliny A, Thomson RL, Nuotio K, Pehlak H, et al. Genetic differentiation in an endangered and strongly philopatric, migrant shorebird. *BMC Ecol Evol*. 2021;21(1):125.
20. Guhlin J, Le Lec MF, Wold J, Koot E, Winter D, Biggs PJ, et al. Species-wide genomics of kākāpō provides tools to accelerate recovery. *Nat Ecol Evol*. 2023;7(10):1693–705.
21. Kardos M, Armstrong EE, Fitzpatrick SW, Hauser S, Hedrick PW, Miller JM, et al. The crucial role of genome-wide genetic variation in conservation. *Proc Natl Acad Sci U S A*. 2021;118(48):e2104642118.
22. Mathur S, Mason AJ, Bradburd GS, Gibbs L. Functional genomic diversity is correlated with neutral genomic diversity in populations of an endangered rattlesnake. *Proc Natl Acad Sci U S A*. 2023;120(43):e2303043120.
23. Gelabert P, Sandoval-Velasco M, Serres A, de Manuel M, Renom P, Margaryan A, et al. Evolutionary history, genomic adaptation to toxic diet, and extinction of the Carolina parakeet. *Curr Biol*. 2020;30(1):108.
24. Guevara EE, Webster TH, Lawler RR, Bradley BJ, Greene LK, Ranaivonasy J, et al. Comparative genomic analysis of sifakas (*Propithecus*) reveals selection for folivory and high heterozygosity despite endangered status. *Sci Adv*. 2021;7(17):eabd2274.
25. Armstrong EE, Khan A, Taylor RW, Gouy A, Greenbaum G, Thiery A, et al. Recent evolutionary history of tigers highlights contrasting roles of genetic drift and selection. *Mol Biol Evol*. 2021;38(6):2366–79.
26. Hogg CJ, Ottewill K, Latch P, Rossetto M, Biggs J, Gilbert A, et al. Threatened species initiative: empowering conservation action using genomic resources. *Proc Natl Acad Sci U S A*. 2022;119(4):e2115643118.
27. Dobrynin P, Liu S, Tamazian G, Xiong Z, Yurchenko AA, Krashennikova K, et al. Genomic legacy of the African cheetah, *Acinonyx jubatus*. *Genome Biol*. 2015;16:277.
28. de Jager D, Glanzmann B, Möller M, Hoal E, van Helden P, Harper C, et al. High diversity, inbreeding and a dynamic Pleistocene demographic history revealed by African buffalo genomes. *Sci Rep*. 2021;11(1):4540.
29. Blair ME. Conservation museomics. *Conserv Biol*. 2024;38(3):e14234.
30. Mikheyev AS, Zwick A, Magrath MJL, Grau ML, Qiu L, Su YN, et al. Museum genomics confirms that the lord howe island stick insect survived extinction. *Curr Biol*. 2017;27(20):3157.
31. Miller W, Hayes VM, Ratan A, Petersen DC, Wittekindt NE, Miller J, et al. Genetic diversity and population structure of the endangered marsupial *Sarcophilus harrisii* (Tasmanian devil). *Proc Natl Acad Sci U S A*. 2012;109(44):18625.
32. Card DC, Shapiro B, Giribet G, Moritz C, Edwards SV. Museum genomics. *Annu Rev Genet*. 2021;55:633–59.
33. Roycroft E, MacDonald AJ, Moritz C, Moussalli A, Miguez RP, Rowe KC. Museum genomics reveals the rapid decline and extinction of Australian rodents since European settlement. *Proc Natl Acad Sci U S A*. 2021;118(27):e2021390118.
34. Bi K, Linderot T, Vanderpool D, Good JM, Nielsen R, Moritz C. Unlocking the vault: Next-generation museum population genomics. *Mol Ecol*. 2013;22(24):6018–32.
35. Dong F, Kuo H-C, Chen G-L, Wu F, Shan P-F, Wang J, et al. Population genomic, climatic and anthropogenic evidence suggest the role of human forces in endangerment of green peafowl (*Pavo muticus*). *Proc Biol Sci*. 1948;2021(288):20210073.
36. Curry CJ, Davis BW, Bertola LD, White PA, Murphy WJ, Derr JN. Spatiotemporal genetic diversity of lions reveals the influence of habitat fragmentation across Africa. *Mol Biol Evol*. 2021;38(1):48–57.
37. Kamp J, Oppel S, Ananin AA, Durnev YA, Gashev SN, Hölzel N, et al. Global population collapse in a superabundant migratory bird and illegal trapping in China. *Conserv Biol*. 2015;29(6):1684–94.
38. Heim W, Chan S, Hoelzel N, Ktitorov P, Mischenko A, Kamp J. East Asian buntings: ongoing illegal trade and encouraging conservation responses. *Conserv Sci Pract*. 2021;3(6):e405.
39. Wang Y, Xue W, Wang H. Save China's yellow-breasted bunting. *Science*. 2019;365(6454):651.
40. Wang P, Hou R, Wu Y, Zhang Z, Que P, Chen P. Genomic status of yellow-breasted bunting following recent rapid population decline. *iScience*. 2022;25(7):104501.
41. Han Z, Zhang L, Jiang Y, Wang H, Jiguet F. Unravelling species co-occurrence in a steppe bird community of Inner Mongolia: insights for the conservation of the endangered Jankowski's bunting. *Divers Distrib*. 2020;26(7):843–52.
42. Wang H, Jiang Y, Gao W. Jankowski's bunting (*Emberiza jankowskii*): current status and conservation. *Chin Birds*. 2010;1(4):251–8.
43. Han Z, Zhang L-S, Qin B, Wang L, Liu Y, Fu VWK, et al. Updated breeding distribution and population status of Jankowski's bunting *Emberiza jankowskii* in China. *Bird Conserv Int*. 2018;28(4):643–52.
44. Han Z, Yang X, Zhang L, Jiguet F, Tryjanowski P, Wang H. Niche overlap between two sympatric steppe birds in Inner Mongolia: habitat selection and insights for conservation. *Ecol Evol*. 2025;15(2):e71010.
45. Li S, Li D, Zhang L, Shang W, Qin B, Jiang Y. High levels of genetic diversity and an absence of genetic structure among breeding populations of the endangered Rufous-backed Bunting in Inner Mongolia, China: implications for conservation. *Avian Res*. 2021;12(7). <https://doi.org/10.1186/s40657-020-00236-3>.
46. Huang L, Feng G, Li D, Shang W, Zhang L, Yan R, et al. Genetic variation of endangered Jankowski's Bunting (*Emberiza jankowskii*): High connectivity and a moderate history of demographic decline. *Front Ecol Evol*. 2023;10:996617.
47. Wang O, Chin R, Cheng X, Wu MKY, Mao Q, Tang J, et al. Efficient and unique cobarcoding of second-generation sequencing reads from long DNA molecules enabling cost-effective and accurate sequencing, haplotyping, and de novo assembly. *Genome Res*. 2019;29(5):798–808.
48. Hughes AR, Inouye BD, Johnson MT, Underwood N, Vellend M. Ecological consequences of genetic diversity. *Ecol Lett*. 2008;11(6):609–23.
49. Ceballos FC, Joshi PK, Clark DW, Ramsay M, Wilson JF. Runs of homozygosity: windows into population history and trait architecture. *Nat Rev Genet*. 2018;19(4):220.
50. Curik I, Ferencakovic M, Soelkner J. Inbreeding and runs of homozygosity: a possible solution to an old problem. *Livest Sci*. 2014;166:26–34.
51. Chen Q, Lin H, Zheng C, Mudrik EA, Kashentseva TA, Cheng Y, et al. Understanding the past to preserve the future: Genomic insights into the conservation management of a critically endangered waterbird. *Mol Ecol*. 2025;34(2):e17606.
52. Nadachowska-Brzyska K, Burri R, Smeds L, Ellegren H. PSMC analysis of effective population sizes in Mol Ecol and its application to black-and-white *Ficedula* flycatchers. *Mol Ecol*. 2016;25(5):1058–72.
53. Liu X, Fu Y-X. Exploring population size changes using SNP frequency spectra. *Nat Genet*. 2015;47(5):555–9.
54. Bertola LV, Higgie M, Zenger KR, Hoskin CJ. Conservation genomics reveals fine-scale population structuring and recent declines in the critically endangered Australian Kuranda Treefrog. *Conserv Genet*. 2023;24(2):249–64.
55. Vandergast AG, Wood DA, Thompson AR, Fisher M, Barrows CW, Grant TJ. Drifting to oblivion? Rapid genetic differentiation in an endangered lizard following habitat fragmentation and drought. *Divers Distrib*. 2016;22(3):344–57.
56. Chen N, Cosgrove EJ, Bowman R, Fitzpatrick JW, Clark AG. Genomic consequences of population decline in the endangered Florida scrub-jay. *Curr Biol*. 2016;26(21):2974–9.

57. Femerling G, van Oosterhout C, Feng S, Bristol RM, Zhang G, Groombridge J, et al. Genetic load and adaptive potential of a recovered avian species that narrowly avoided extinction. *Mol Biol Evol.* 2023;40(12):msad256.
58. Huang L, Zhang L, Li D, Yan R, Shang W, Jiang Y, et al. Molecular evidence of introgressive hybridization between related species Jankowski's Bunting (*Emberiza jankowskii*) and Meadow Bunting (*Emberiza cioides*) (Aves: Passeriformes). *Avian Res.* 2022. <https://doi.org/10.1016/j.avrs.2022.100035>.
59. Schmidt C, Hoban S, Hunter M, Paz-Vinas I, Garraway CJ. Genetic diversity and IUCN red list status. *Conserv Biol.* 2023;37(4):e14064.
60. Willoughby JR, Sundaram M, Wijayawardena BK, Kimble SJA, Ji Y, Fernandez NB, et al. The reduction of genetic diversity in threatened vertebrates and new recommendations regarding IUCN conservation rankings. *Biol Conserv.* 2015;191:495–503.
61. Murray GGR, Soares AER, Novak BJ, Schaefer NK, Cahill JA, Baker AJ, et al. Natural selection shaped the rise and fall of passenger pigeon genomic diversity. *Science.* 2017;358(6365):951–4.
62. Hung C-M, Shaner P-JL, Zink RM, Liu W-C, Chu T-C, Huang W-S, et al. Drastic population fluctuations explain the rapid extinction of the passenger pigeon. *Proc Natl Acad Sci U S A.* 2014;111(29):10636–41.
63. Roos C, Seshadri L, Zhang L, Harris RA, Raveendran M, Cuadros Espinoza SH, et al. Genomic basis of non-human-primate diversity and adaptation. *Nat Rev Biodivers.* 2025;1:353–70.
64. Robinson JA, Bowie RCK, Dudchenko O, Aiden EL, Hendrickson SL, Steiner CC, et al. Genome-wide diversity in the California condor tracks its prehistoric abundance and decline. *Curr Biol.* 2021;31(13):2939.
65. Byerly PA, Chesser RT, Fleischer RC, McInerney N, Przelomska NAS, Leberg PL. Museum genomics provide evidence for persistent genetic differentiation in a threatened seabird species in the western Atlantic. *Integr Comp Biol.* 2022;62(6):1838–48.
66. Salado I, Preick M, Lupianez-Corpas N, Fernandez-Gil A, Vila C, Hofreiter M, et al. Loss of mitochondrial genetic diversity despite population growth: the legacy of past wolf population declines. *Genes.* 2022;14(1):75.
67. Stoffel MA, Johnston SE, Pilkington JG, Pemberton JM. Genetic architecture and lifetime dynamics of inbreeding depression in a wild mammal. *Nat Commun.* 2021;12(1):2972.
68. Hill EW, McGivney BA, MacHugh DE. Inbreeding depression and durability in the North American Thoroughbred horse. *Anim Genet.* 2023;54(3):408–11.
69. Tsheten G, Fuerst-Waltl B, Pfeiffer C, Soelkner J, Bovenhuis H, Meszaros G. Inbreeding depression and its effect on sperm quality traits in Pietrain pigs. *J Anim Breed Genet.* 2023;140(6):653–62.
70. Khan A, Patel K, Shukla H, Viswanathan A, van der Valk T, Borthakur U, et al. Genomic evidence for inbreeding depression and purging of deleterious genetic variation in Indian tigers. *Proc Natl Acad Sci U S A.* 2021;118(49):e2023018118.
71. Harrison KA, Magrath MJL, Yen JDL, Pavlova A, Murray N, Quin B, et al. Lifetime fitness costs of inbreeding and being inbred in a critically endangered bird. *Curr Biol.* 2019;29(16):2711.
72. Hasselgren M, Dussex N, von Seth J, Angerbjorn A, Dalen L, Noren K. Strongly deleterious mutations influence reproductive output and longevity in an endangered population. *Nat Commun.* 2024;15(1):1–10.
73. Luo R, Liu B, Xie Y, Li Z, Huang W, Yuan J, et al. SOAPdenovo2: an empirically improved memory-efficient short-read de novo assembler. *Gigascience.* 2012;1(1):18.
74. Weisenfeld NI, Kumar V, Shah P, Church DM, Jaffe DB. Direct determination of diploid genome sequences. *Genome Res.* 2017;27(5):757–67.
75. Xu GC, Xu TJ, Zhu R, Zhang Y, Li SQ, Wang HW, et al. Lr_gapcloser: a tiling path-based gap closer that uses long reads to complete genome assembly. *Gigascience.* 2019;8(1):giy157.
76. Seppy M, Manni M, Zdobnov EM. BUSCO: assessing genome assembly and annotation completeness. *Methods Mol Biol.* 2019;1962:227–45.
77. Manni M, Berkeley MR, Seppy M, Simão FA, Zdobnov EM. BUSCO update: novel and streamlined workflows along with broader and deeper phylogenetic coverage for scoring of eukaryotic, prokaryotic, and viral genomes. *Mol Biol Evol.* 2021;38(10):4647–54.
78. Chen S, Zhou Y, Chen Y, Gu J. Fastp: an ultra-fast all-in-one FASTQ preprocessor. *Bioinformatics.* 2018;34(17):884–90.
79. Zhang D, She H, Wang S, et al. Phylogenetic conflict between species tree and maternally inherited gene trees in a clade of *Emberiza* buntings (Aves: Emberizidae). *Syst Biol.* 2024;73(2):279–89.
80. Zhang D, She H, Rheindt FE, Wu L, Wang H, Zhang K, et al. Genomic and phenotypic changes associated with alterations of migratory behaviour in a songbird. *Mol Ecol.* 2023;32(2):381–92.
81. Cai T, Wu G, Sun L, Zhang Y, Peng Z, Guo Y, et al. Biogeography and diversification of old world buntings (Aves: Emberizidae): radiation in open habitats. *J Avian Biol.* 2021. <https://doi.org/10.1111/jav.02672>.
82. Li H, Durbin R. Fast and accurate short read alignment with Burrows-Wheeler transform. *Bioinformatics.* 2009;25(14):1754–60.
83. Quinlan AR, Hall IM. BEDtools: a flexible suite of utilities for comparing genomic features. *Bioinformatics.* 2010;26(6):841–2.
84. Li H, Handsaker B, Wysoker A, Fennell T, Ruan J, Homer N, et al. The sequence alignment/map format and SAMtools. *Bioinformatics.* 2009;25(16):2078–9.
85. Danecek P, Auton A, Abecasis G, Albers CA, Banks E, DePristo MA, et al. The variant call format and VCFtools. *Bioinformatics.* 2011;27(15):2156–8.
86. Zhang C, Dong S-S, Xu J-Y, He W-M, Yang T-L. Poplddecay: a fast and effective tool for linkage disequilibrium decay analysis based on variant call format files. *Bioinformatics.* 2019;35(10):1786–8.
87. Howrigan DP, Simonson MA, Keller MC. Detecting autozygosity through runs of homozygosity: a comparison of three autozygosity detection algorithms. *BMC Genomics.* 2011;12:460.
88. Li H, Durbin R. Inference of human population history from individual whole-genome sequences. *Nature.* 2011;475(7357):493–6.
89. Nadachowska-Brzyska K, Konczal M, Babik W. Navigating the temporal continuum of effective population size. *Methods Ecol Evol.* 2022;13(1):22–41.
90. Lu S, Liu L, Lei W, Wang D, Zhu H, Lai Q, et al. Cryptic divergence in and evolutionary dynamics of endangered hybrid *Picea brachytyla* sensu stricto in the Qinghai-Tibet Plateau. *BMC Plant Biol.* 2024;24(1):1202.
91. Korneliussen TS, Albrechtsen A, Nielsen R. ANGSD: analysis of next generation sequencing data. *BMC Bioinformatics.* 2014;15(1):356.
92. Wang S. Genomes of *Emberiza aureola* and *Emberiza jankowskii*. 2025. CNGB <https://doi.org/10.26036/CNP0007710>.
93. Wang S. Whole genome of five species in *Emberiza*. GenBank. 2025. <http://identifiers.org/ncbiprotein:PRJNA1264757>.

Publisher's Note

Springer Nature remains neutral with regard to jurisdictional claims in published maps and institutional affiliations.